PRAMANA
— journal of
physics

Vol. 75, No. 6
December 2010
pp. 1041–1056

An overview of some experimental and theoretical aspects of fundamental symmetry violations in atoms

D BUDKER[1,*], B K SAHOO[2], D ANGOM[2] and B P DAS[3]
[1]Department of Physics, University of California at Berkeley, Berkeley, California 94720-7300, USA
[2]Theoretical Physics Division, Physical Research Laboratory, Ahmedabad 380 009, India
[3]Indian Institute of Astrophysics, Bangalore 560 034, India
[*]Corresponding author. E-mail: budker@berkeley.edu

Abstract. We present some of the advances in our experimental and theoretical studies of violations in fundamental symmetries in atoms. A part of this work was performed under the auspices of a NSF–DST project. During this period, a number of experimental techniques and theoretical methods were developed and employed for precision measurements and their interpretation from first principles. Future directions of these studies are briefly mentioned.

Keywords. Parity violation; polarizability; spectroscopy; Bose–Einstein statistics.

PACS Nos 31.15.-p; 32.10.-f

1. Introduction

The long-term scientific collaboration between the Berkeley experimental group led by one of the authors (DB) and the Indian theoretical group led by another (BPD), was put on a solid basis by the support from a joint NSF–DST program. This support resulted in numerous research visits between Berkeley and India, involving researchers at all levels – from graduate students to principal investigators. In this paper, we briefly summarize the results of the work in the area of testing fundamental symmetries of Nature that were obtained during the course of the collaboration and exchanges.

Space inversion (P) is one of the fundamental discrete symmetries of Nature. It is violated maximally in the weak interactions and the observation of parity nonconservation (PNC) is an important probe to validate the predictions of the Standard Model of particle physics. In this regard, the atomic PNC experiments have a long history of providing unique tests of the Standard Model of particle physics [1]. These are low-energy probes of phenomena which occur at several TeV and complement the accelerator-based experiments. One guiding principle in the

choice of candidate atoms is the Z^3 dependence of the PNC effects in atoms [2]. Heavy atoms in general and Yb in particular are therefore the preferred candidates to study these effects. The special features of PNC in Yb have been highlighted by DeMille [3]. Theoretical work [3–5] has predicted that the effect in Yb should be $\approx$100$\times$ larger than that in Cs. Recently, an experiment at Berkeley [6,7] has confirmed this prediction. In addition, Yb has many stable isotopes, making it possible to perform an isotopic comparison of the PNC effect. Using an isotopic comparison to extract information on the Standard Model overcomes the uncertainties arising from atomic theory. However, atomic theory is still needed to extract the value of nuclear anapole moment. In addition, to assess the level of precision achieved in the atomic PNC calculations, it is essential to study other related properties like dipole polarizabilities, hyperfine interactions and allowed transition amplitudes. A comparison of the theoretical and experimental results of these quantities helps to quantify the accuracy of the atomic calculations. Besides atomic Yb, PNC effects have also been studied in atomic Dy [8]. Atomic Dy is also a suitable candidate to measure temporal variation of the fine structure constant α. This was theoretically proposed by Flambaum and coworkers [9] and was experimentally measured at Berkeley [10].

Permutation symmetry of the wave functions of a quantum system, consisting of identical and indistinguishable particles, is related to the quantum statistics. One may test the Bose–Einstein statistics, which describes bosons, with Landau–Yang theorem [11,12] in the two-photon atomic transitions. At Berkeley, experimental work with Ba began with the goal of providing a stringent test of Bose–Einstein statistics for photons [13]. During this work we have measured polarizabilities of numerous states. The Landau–Yang theorem is applied to the decay of atomic states and elementary particles. One generalization of Landau–Yang theorem is the decay process in the presence of external fields, which is the case in most of the physical systems of interest. In the atomic experiments, other static fields are present in the apparatus, and other fields are there in the decay of elementary particles. This was examined in one of the theoretical investigations [14].

The remaining part of the paper is organized as follows: In the following section, we discuss the experimental advances made during this project. We then discuss the theoretical studies on the atomic structure of ytterbium (Yb), following which we give a theoretical formulation to evaluate static polarizabilities of the ground states of many atoms including Ba and Yb. Determination of other properties including AC Stark shift in Yb is presented and discussed thereafter.

2. Atomic parity violation

2.1 *Yb*

The Yb parity-violation experiment utilizes a collimated atomic beam. The atoms in the beam pass consecutively through two interaction regions. In the first interaction region, the atoms are exposed to light at 408 nm that is resonant with the $^1S_0 \rightarrow {}^3D_1$ parity-forbidden transition. The light is produced by frequency-doubling the output of a Ti-sapphire laser. The intensity of the 408 nm light is

enhanced in an in-vacuum power-build-up optical cavity. The light–atom interaction in the first interaction region occurs in the presence of orthogonal electric and magnetic fields (**E** and **B**, respectively) applied by means of appropriate electrodes and coils. The electric field is necessary to supply the reference Stark-induced transition amplitude, whereas the magnetic field separates the Zeeman components of the transition, which is necessary to avoid the cancellation of the parity-violation effect. The geometry can be understood by considering the rotational invariant that corresponds to the parity-violation effect: the signal due to this effect scales as

$$(\boldsymbol{\epsilon} \cdot \mathbf{B})(\boldsymbol{\epsilon} \cdot \mathbf{E} \times \mathbf{B}), \tag{1}$$

where $\boldsymbol{\epsilon}$ is the light polarization vector. It is easy to see that this quantity changes sign upon spatial inversion but remains invariant under the reversal of time.

By exciting to the upper $^3D_1$ state of the forbidden transition, the atoms decay, with $\approx$70% probability to the metastable $^3P_0$ state. It is in this state that they travel to the second interaction region where they are detected with high efficiency by re-exciting them to the $^3S_1$ state, and collecting and detecting the ensuing cascade fluorescence. The experiments have yielded results [6,7] corresponding to the largest parity-violation effect observed so far, in agreement with theoretical expectations [3–5].

There are theoretical issues in conjunction with this experiment that require careful study. The foremost issue is perhaps the sign mismatch between two theoretical results, [5] and [15], of the atomic PNC arising from the nuclear anaploe moment. It is important to resolve this discrepancy to analyse the experimental results and obtain bounds on the nuclear anapole moment. In a recent work, a Fock-space coupled-cluster theory-based method was developed to calculate the structure and properties of two-valence systems like atomic Yb [16]. Indeed, calculating the PNC of Yb with improved accuracy is the motivation for developing the method.

Accurate calculations of atomic structure and properties, at a level commensurate with the experimental data, is a theoretical challenge, especially for the high Z atoms of interest in atomic PNC experiments and Yb is no exception. Theoretically, there are standard ways, like different gauges in transition amplitude calculations, to check the accuracy of the atomic calculations. A convincing and more direct approach however, is to reproduce experimental data with *ab-initio* atomic theory calculations. This is possible with the results obtained from the precision experimental measurements in the context of atomic PNC observation [17,18]. This is equivalent to testing the reliability of the state-of-the-art atomic many-body theories and schemes of calculations.

Another, perhaps indirect, important outcome is the possibility to check the neutron distribution. Although it is possible to probe the proton distribution in nuclei from μ scattering through electromagnetic interaction, there is no direct way to measure neutron distribution through scattering experiments and isotope shifts. The atomic PNC experiments, which detect signatures of electron–nucleus weak interactions, can probe the neutron density distributions [19]. Thus, atomic PNC can provide valuable insights to fine tune and check nuclear models. PNC measurements of the seven Yb isotopes offer the unique possibility of examining variation in the neutron density across an isotope chain.

2.2 *Dy*

The dysprosium (Dy) system has drawn attention in 1986 [20] because there are nearly degenerate states of opposite nominal parity and the same total electronic angular momentum. With Dy being a heavy atom (atomic number $Z = 66$), there was hope that parity-violation effects in this system would be very large. This expectation was confirmed by early theoretical estimates. Unfortunately, early experimental studies showed that the effect was not as large as initially expected [8]. A recent calculation by Dzuba *et al* [21] puts the expected effect just below the experimental limit.

In the meantime, it was pointed out by Flambaum *et al* that the Dy system is a very efficient system to search for a possible variation of the fine-structure constant α, which led to successful experimental efforts at Berkeley [10,22,23]. The dysprosium experiment also involves an atomic-beam apparatus. The odd-parity state of the nearly degenerate states of interest for both the parity-violation measurements and the variation-of-α experiment is populated using a sequence of three consecutive transitions (two laser-driven and one spontaneous) [24]. The radiofrequency transitions between the nearly degenerate opposite-parity states are induced in the interaction region, where the population of the shorter-lived even-parity states is monitored by detecting the cascade fluorescence. Significant enhancement of the experimental sensitivity and improved control of systematic effects is expected from the second-generation apparatus, now fully operational and taking data, as well as from transverse laser cooling of the dysprosium atoms in the beam recently demonstrated at Berkeley [25–27] for all stable isotopes of Dy (including the ones with nonzero nuclear spin). The new-generation experiment, presently accumulating data, combines the search for temporal variation of α with the measurement of parity violation, both at levels of sensitivity significantly better than the earlier respective experiments.

3. Test of quantum statistics with Ba

According to Landau–Yang theorem [11,12], an initial $J = 1$ state cannot decay into two photons. The theorem is very general and applicable to a wide range of phenomena from atomic physics to elementary particle physics. The main ingredients of the proof lies in the fact that the initial $J = 1$ state gives us a vector to specify the initial state of the decaying particle and the final photons have their polarization vectors to specify their conditions. It turns out that there is no way in which one can write a decay amplitude of the neutral vector particle to two photons such that the final photons are transverse and the amplitude remains symmetric under their interchange.

The experimental test of the theorem underway at Berkeley is using a collimated atomic beam of barium, similar to the one in the Yb parity-violation experiment. Similar to the Yb experiment, the Ba atoms also interact with laser light in an in-vacuum power build-up cavity. In this case, however, the outputs of two independent dye lasers are coupled to the cavity (their frequency is locked to the cavity using the Pound–Drever–Hall technique). The two lasers can either be locked to the

same longitudinal mode of the cavity to attempt to drive the forbidden two-photon transition, or to two distinct modes in order to drive the same transition, which is now allowed because the photons from the two lasers are no longer degenerate. In both cases, the sum of the frequencies of the light from the two lasers is scanned through the two-photon resonance. As in the Yb and Dy experiments, transition can be detected by observing fluorescence.

The experiment has resulted not only in the new stringent limit on possible violation of Bose statistics by photons [28], but also in the observation (and a theoretical analysis) of hyperfine-interaction enabled forbidden two-photon transitions [29].

An extension of the theorem, which has wider applications, is the modifications in the presence of external fields. One scenario is to investigate the decay of neutral spin-one particle in the presence of a uniform classical background magnetic field. If the initial decaying particle has a magnetic moment then it can interact with the magnetic field. Even if the initial particle does not have any magnetic moment, magnetic fields can still enter into the scenario through their interaction with virtual charged fermions or other charged particles propagating in the loops which accompany the Feynman diagram of the decay process. There are many calculations as for example the photon self-energy or photon pair creation in a magnetic field employing suitable fermion propagators [30]. In the presence of an external magnetic field we can in general have 15 candidates for the decay amplitude. The number of candidates reduces to nine if we apply other symmetries like CP and the resultant decay amplitude shows anisotropic features [14].

4. Atomic Yb structure calculations

4.1 *Valence correlation effects*

The low-lying levels of atomic Yb given in figure 1 are important for the studies related to parity-violating effects. In the calculations reported, the single electron wave functions or orbitals generated in a sequence of multi-configuration Dirac–Fock (MCDF) self-consistent field calculations with a limited configuration space. The orbital space consists of (1-5)s, (2-5)p, (3-4)d and $4f$ as core; $5d$, $6s$ and $6p$ as valence; the remaining (7-9)s, (7-9)p, (6-9)d, (6-9)f and (7-9)g as virtual. The core and valence orbitals are generated in a single calculation and the virtual orbitals of the same principal quantum number or layer are generated together. The single-particle orbitals generated using GRASP [31] and their orbital energies are given in table 1.

The multiconfiguration Dirac–Fock calculations in general include the most important electron correlation effects. These effects can be taken into account more accurately by performing large-scale configuration interaction calculations of the atomic states that are needed to calculate a particular property. The electron correlation has three sectors: core–core, core–valence and valence–valence. Each of these can be studied by an appropriate choice of the configuration space in a configuration interaction calculation. All these three cases have been studied for Yb in a series of calculations.

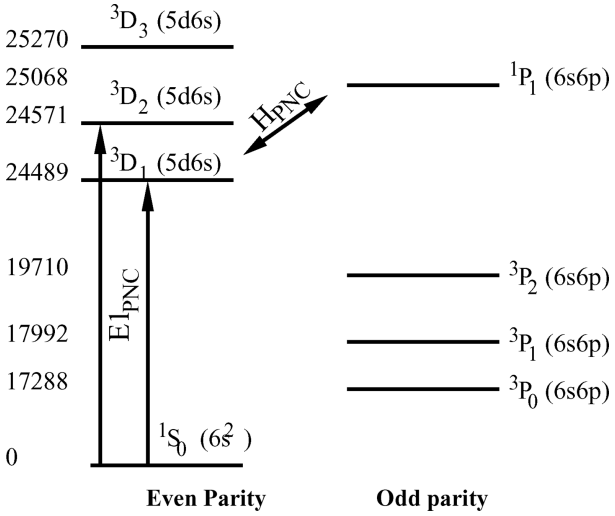

Figure 1. The low-lying energy levels (in cm^{-1}) of atomic Yb. The double arrow represents the H_{PNC} mixing and single arrow represents the transitions of interest for $E1_{\mathrm{PNC}}$ measurement.

Table 1. The energies of the orbitals in atomic units.

Orbital	ϵ	Orbital	ϵ	Orbital	ϵ	Orbital	ϵ
1s	−2267.671	$5s$	−2.460	$7s$	−0.232	$8f_{5/2}$	−0.248
2s	−388.915	$5p_{1/2}$	−1.447	$7p_{1/2}$	−0.165	$8f_{7/2}$	−0.256
$2p_{1/2}$	−370.075	$5p_{3/2}$	−1.210	$7p_{3/2}$	−0.169	$8g_{7/2}$	−0.225
$2p_{3/2}$	−331.507	$4f_{5/2}$	−0.558	$7d_{3/2}$	−0.279	$8g_{9/2}$	−0.226
$3s$	−89.729	$4f_{7/2}$	−0.500	$7d_{5/2}$	−0.250	$9s$	−0.228
$3p_{1/2}$	−81.442	$5d_{3/2}$	−0.112	$7f_{5/2}$	−0.260	$9p_{1/2}$	−0.196
$3p_{3/2}$	−73.114	$5d_{5/2}$	−0.115	$7f_{7/2}$	−0.260	$9p_{3/2}$	−0.212
$3d_{3/2}$	−59.211	$6s$	−0.237	$7g_{7/2}$	−0.226	$9d_{3/2}$	−0.204
$3d_{5/2}$	−57.410	$6p_{1/2}$	−0.156	$7g_{9/2}$	−0.225	$9d_{5/2}$	−0.176
$4s$	−18.689	$6p_{3/2}$	−0.149	$8s$	−0.240	$9f_{5/2}$	−0.288
$4p_{1/2}$	−15.288	$6d_{3/2}$	−0.239	$8p_{1/2}$	−0.204	$9f_{7/2}$	−0.257
$4p_{3/2}$	−13.386	$6d_{5/2}$	−0.259	$8p_{3/2}$	−0.191	$9g_{7/2}$	−0.226
$4d_{3/2}$	−7.798	$6f_{5/2}$	−0.229	$8d_{3/2}$	−0.236	$9g_{9/2}$	−0.225
$4d_{5/2}$	−7.442	$6f_{7/2}$	−0.226	$8d_{5/2}$	−0.222		

To study the valence–valence correlation effects, the configuration space chosen has single and double replacements from the valence to the virtual shells. This is done in a series of calculations, in which one layer of virtual orbitals is added in each calculation. The last in the series has 1294 configuration state functions and the excitation energies calculated are given in table 2. The $5d6s\ ^3D_2$ and $6s6p\ ^3P_0$ levels have 0.2% and 17% minimum and maximum deviations, respectively from the experimental data. In addition, there is a discrepancy between the theoretical level

Table 2. The calculated excitation energies $E_{\rm Th}$ and the experimental data $E_{\rm Exp}$ in Kaysers. For comparison, the differences $\delta E = E_{\rm Th} - E_{\rm Exp}$ are also given. The $6s6p$ and $5d6s$ multiplets exhibit opposite deviations from the experimental data.

	Excitation energies		Diff(δE)
Level	$E_{\rm Th}$	$E_{\rm Exp}$	$E_{\rm Th} - E_{\rm Exp}$
$6s6p\ ^3P_0$	14326	17288	−2962
$6s6p\ ^3P_1$	14985	17992	−3007
$6s6p\ ^3P_2$	16487	19710	−3223
$6s6p\ ^1P_1$	24177	25068	−891
$5d6s\ ^3D_1$	25227	24489	738
$5d6s\ ^3D_2$	25251	24752	499
$5d6s\ ^3D_2$	25324	25271	53

sequence and experimental data. The calculated $6s6p\ ^1P_1$ lies below the $5d6s\ ^3D_J$ multiplets, but from the experimental data it should lie between $5d6s\ ^3D_2$ and $5d6s\ ^3D_3$. The discrepancy could be a consequence of the correlation effects not included in the calculations.

4.2 *Core polarization effects*

The core–valence correlation sector or core-polarization effect is an important contribution not included in the previous series of configuration interaction calculations. This is included when configurations with replacements from the core and valence shells are part of the configuration space. In the present work, the effect of polarizing the $4d$, $5s$, $5p$ and $4f$ core shells were studied systematically. For the level of precision required, the contributions from the deeper core shells can be neglected. The core shells to be included is chosen after test calculations.

Initial or test calculations with the orbital (1-7)s, (2-7)p, (3-7)d, (4-7)f and $7g$ were done to estimate the polarization effects of the core orbitals. That is, the orbital space has only one layer of virtual orbitals. It is to be noted, based on the multipole selection in the inter-electron Coulomb interaction that core orbital of angular momentum l has dominant contribution from the virtual orbitals of orbital angular momenta l and $l \pm 1$. Hence, the inclusion of $7g$ is essential to get correct core polarization effects of $4f$. The results are given in table 3. Among the core shells studied, the $4f$ and $5p$ core shells have large contributions. For the deeper core shells, the effect of $4d$ and below are negligible. This can be explained in terms of perturbative expansion, in which the increasing ionization energy of the deeper core shells suppresses the contribution. Large contribution from $4f$ and $5p$ is expected because the energy separation of $4f$ and $5p$ from the valence shells is small. From the observed trend it is sufficient to consider $4f$, $5p$ and $5s$. There are two important results in the calculations. First, the $5p$ core-polarization effect

Table 3. The core–valence correlation sector or the core-polarization effects from the $4f$, $5p$, $5s$ and $4d$ core shells. The core shells are excited in steps, and in the table, the first column lists the core shells excited and δE is the change in the excitation energy from the previous result.

Core shells excited	$6s6p$				$5d6s$		
	$^3P_0$	$^3P_1$	$^3P_2$	$^1P_1$	$^3D_1$	$^3D_1$	$^3D_1$
	14264	14924	16426	24174	25218	25239	25308
$4f$	14831	15496	17050	23938	24320	24404	24552
δE	567	572	624	−236	−898	−835	−756
$4f$, $5p$	15676	16352	17967	24398	23537	23635	23807
δE	845	856	917	460	−783	−769	−745
$4f$, $5f$, $5s$	15693	16370	17989	24430	23468	23567	23744
δE	17	18	22	32	−69	−68	−63
$4f$, $5f$, $5s$, $4d$	15693	16370	17990	24429	23461	23561	23739
δE	0	0	1	−1	−7	−6	−5

lifts the $6s6p\ ^1P_1$ above the $5d6s$ multiplets. This takes the level sequence closer to the experimental data but not the same. In the experimental data $6s6p\ ^1P_1$ lies between $5d6s\ ^3D_2$ and $5d6s\ ^3D_3$. Second $5s$ and $5p$ produces a different shift to $6s6p\ ^1P_1$ in comparison to $4f$ and $4d$.

4.3 *Core–core correlation effects*

The core–core correlation effects are calculated by including configurations with double excitations from the core shells in the configuration space. The results of $4f$ core–core correlation effects are given in table 4. The results show that the contribution of $4f$–$4f$ core correlation effects is minimal. The changes are in the same range as in the core–polarization contribution from $5s$.

5. Static polarizability calculations

Calculations of atomic polarizabilities have come a long way since the classic work of Dalgarno and Lewis [32]. A few calculations of the polarizabilities of heavy atomic systems have been performed in the past few years using the linearized as well as the non-linearized relativistic coupled-cluster (RCC) theory. These are based on approaches that sum over a set of intermediate states. There has been considerable interest in accurate calculations of the dipole polarizabilities of alkaline-earth atoms and Yb [33–39]. We have given an approach [40] to calculate the polarizabilities of the ground states in these systems by avoiding the usual sum-over-states approach by solving the perturbed RCC wave function to first order in the dipole and all orders in the residual Coulomb interaction that has been discussed here.

Table 4. The contribution from the configurations with double excitations from the $4f$ shell. The column *Without* and *With* are the excitation energies without and with double excitations from the $4f$ shell.

	Excitation energies		
Level	Without	With	Change
$6s6p\ ^3P_0$	14664	14698	−34
$6s6p\ ^3P_1$	15327	15362	−35
$6s6p\ ^3P_2$	16877	16917	−40
$5d6s\ ^3D_1$	23695	23612	83
$5d6s\ ^3D_2$	23804	23724	80
$5d6s\ ^3D_3$	24001	23923	178
$6s6p\ ^1P_1$	23824	23992	−168

In a uniform DC electric field $\mathbf{E} = \mathcal{E}\hat{\mathbf{z}}$, the energy shift ΔE of the ground state $|\Psi_0^{(0)}(\pi, J_0, M_0)\rangle$ with the parity eigenvalue π and angular momentum $J_0 = 0$ and its azimuthal value $M_0 = 0$ is given by

$$\Delta E = -\frac{1}{2}\alpha\mathcal{E}^2, \tag{2}$$

where α is the static polarizability and can be expressed as

$$\alpha = -2\sum_I \frac{|\langle\Psi_0^{(0)}(\pi, J_0, M_0)|D_z|\Psi_I^{(0)}(\pi', J_I, M_I)\rangle|^2}{E_0 - E_I}, \tag{3}$$

where subscript 0 and I represent ground and excited states of the Dirac–Coulomb (DC) Hamiltonian ($H_0^{(\mathrm{DC})}$), respectively, the superscript (0) represents unperturbed wave functions, D_z is the zth component of the electric dipole operator, J_I, M_I are the angular momentum quantum numbers of the intermediate states, π and π' are the parity quantum numbers for states of opposite parity and E_0 and E_I are the energies of the ground and intermediate states, respectively.

In a more explicit form, the above expression can be written as

$$\begin{aligned}\alpha &= \langle\Psi_0^{(0)}(\pi, J_0, M_0)|D_z|\Psi_0^{(1)}(\pi', J', M')\rangle \\ &\quad + \langle\Psi_0^{(1)}(\pi', J', M')|D_z|\Psi_0^{(0)}(\pi, J_0, M_0)\rangle \\ &= \langle\Psi_0|D_z|\Psi_0\rangle,\end{aligned} \tag{4}$$

where

$$|\Psi_0\rangle = |\Psi_0^{(0)}(\pi, J_0, M_0)\rangle + |\Psi_0^{(1)}(\pi', J', M')\rangle, \tag{5}$$

with $|\Psi_0^{(1)}(\pi', J', M')\rangle$ as the first-order correction with the angular momentum $J'(= 1)$ and M' due to the operator D_z to the original unperturbed wave function, $|\Psi_0^{(0)}(\pi, J_0, M_0)\rangle$, in the presence of an external electric field and given by

$$|\Psi_0^{(1)}(\pi', J', M')\rangle = \sum_I |\Psi_I^{(0)}(\pi', J_I, M_I)\rangle \times \frac{\langle\Psi_I^{(0)}(\pi', J_I, M_I)|D_z|\Psi_0^{(0)}(\pi, J_0, M_0)\rangle}{E_0 - E_I} \times\delta(J', J_I)\delta(M', M_I)\delta(M_0, M_I). \quad (6)$$

The first-order perturbed wave function $|\Psi_0^{(1)}(\pi', J', M')\rangle$ can be obtained using an approach that explicitly avoids summing over intermediate states.

Using the CC ansatz, the all-order unperturbed wave function $|\Psi_0^{(0)}(\pi, J_0, M_0)\rangle$ for closed-shell atoms can be expressed as

$$|\Psi_0^{(0)}(\pi, J_0, M_0)\rangle = \mathrm{e}^{T^{(0)}}|\Phi_0(\pi, J_0, M_0)\rangle, \quad (7)$$

where $|\Phi_0(\pi, J_0, M_0)\rangle$ are the Dirac–Fock (DF) wave functions determined using the mean-field approximation and $T^{(0)}$ are the electron excitation operators due to Coulomb interaction from the corresponding DF states.

To obtain $|\Psi_0^{(1)}(\pi', J', M')\rangle$, we proceed as follows:

Let us operate $(H_0^{(\mathrm{DC})} - E_0)$ on both sides of eq. (6), i.e.

$$\begin{aligned}(H_0^{(\mathrm{DC})} - E_0)|\Psi_0^{(1)}(\pi', J', M')\rangle &= \sum_I (H_0^{(\mathrm{DC})} - E_0)|\Psi_I^{(0)}(\pi', J_I, M_I)\rangle \times \frac{\langle\Psi_I^{(0)}(\pi', J_I, M_I)|D_z|\Psi_0^{(0)}(\pi, J_0, M_0)\rangle}{E_0 - E_I} \\ &= \sum_I (E_I - E_0)|\Psi_I^{(0)}(\pi', J_I, M_I)\rangle \times \frac{\langle\Psi_I^{(0)}(\pi', J_I, M_I)|D_z|\Psi_0^{(0)}(\pi, J_0, M_0)\rangle}{E_0 - E_I} \\ &= -\sum_I |\Psi_I^{(0)}(\pi', J_I, M_I)\rangle \times\langle\Psi_I^{(0)}(\pi', J_I, M_I)|D_z|\Psi_0^{(0)}(\pi, J_0, M_0)\rangle. \end{aligned} \quad (8)$$

Using the completeness principle of the atomic states of the DC Hamiltonian, $\sum_\alpha |\Psi_\alpha^{(0)}\rangle\langle\Psi_\alpha^{(0)}| = 1$, we get

$$\sum_I |\Psi_I^{(0)}(\pi', J_I, M_I)\rangle\langle\Psi_I^{(0)}(\pi', J_I, M_I)| = 1 - \sum_{K\neq I} |\Psi_K^{(0)}(\pi, J_K, M_K)\rangle \times\langle\Psi_K^{(0)}(\pi, J_K, M_K)|. \quad (9)$$

Substituting eq. (9) in eq. (8), we get

$$\begin{aligned}(H_0^{(\mathrm{DC})} - E_0)|\Psi_0^{(1)}(\pi', J', M')\rangle &= -D_z|\Psi_0^{(0)}(\pi, J_0, M_0)\rangle \\ &\quad + \sum_K |\Psi_K^{(0)}(\pi, J_K, M_K)\rangle\langle\Psi_K^{(0)}(\pi, J_K, M_K)|D_z|\Psi_0^{(0)}(\pi, J_0, M_0)\rangle \\ &= -D_z|\Psi_0^{(0)}(\pi, J_0, M_0)\rangle, \end{aligned} \quad (10)$$

where the second term does not contribute because $|\Psi_K^{(0)}(\pi, J_K, M_K)\rangle$ and $|\Psi_0^{(0)}(\pi, J_0, M_0)\rangle$ have the same parity.

The above equation represents a first-order perturbed equation with D_z as the perturbation and the first-order energy is equal to zero. The unperturbed wave function is represented by $|\Psi_0^{(0)}(\pi, J_0, M_0)\rangle$ and $|\Psi_0^{(1)}(\pi', J', M')\rangle$ is its first-order correction. In order to obtain the solution for $|\Psi_0^{(1)}(\pi', J', M')\rangle$, we solve eq. (10) using the following (R)CC approach.

Using the above CC ansatz for closed-shell atoms, we can express the total wave function $|\Psi_0\rangle$, which is of mixed parity and angular momentum, by

$$|\Psi_0\rangle = \mathrm{e}^T |\Phi_0(\pi, J_0, M_0)\rangle, \tag{11}$$

where we now define

$$T = T^{(0)} + T^{(1)}, \tag{12}$$

with $T^{(1)}$ representing the excitation operators containing all orders in the Coulomb interaction and one order in D_z. Substituting eq. (12) in eq. (11), we get

$$\begin{aligned} |\Psi_0\rangle &= \mathrm{e}^{T^{(0)}+T^{(1)}} |\Phi_0(\pi, J_0, M_0)\rangle \\ &= \mathrm{e}^{T^{(0)}} (1 + T^{(1)}) |\Phi_0(\pi, J_0, M_0)\rangle, \end{aligned} \tag{13}$$

where only terms up to linear in $T^{(1)}$ (i.e. those terms up to one order in D_z) are retained.

It is clear from eq. (13) that the first-order perturbed wave function can now be written as

$$|\Psi_0^{(1)}(\pi', J', M')\rangle = \mathrm{e}^{T^{(0)}} T^{(1)} |\Phi_0(\pi, J_0, M_0)\rangle. \tag{14}$$

The $T^{(1)}$ amplitudes are determined using the following equations:

$$\langle \Phi_0^* | \overline{H_0^{(\mathrm{DC})}} T^{(1)} | \Phi_0 \rangle = -\langle \Phi_0^* | \overline{D_z} | \Phi_0 \rangle, \tag{15}$$

where we have used the relation $\overline{O} = \mathrm{e}^{-T^{(0)}} O \mathrm{e}^{T^{(0)}} = ((O\mathrm{e}^{T^{(0)}})_{\mathrm{con}}$.

We have considered only the singly and doubly excited states (known as CCSD method) denoted by T_1 and T_2, respectively, with the appropriate superscripts in these calculations. However, we have estimated contributions from the neglected triple excitations by constructing the corresponding triple excitation operators from the contraction between T_2 and $H_0^{(\mathrm{DC})}$. These contributions are treated as possible error bars for CCSD results.

Using eqs (7) and (14), the expression for the polarizabilities using the (R)CC operators can be expressed as

$$\begin{aligned} \alpha &= \frac{\langle \Phi_0 | \mathrm{e}^{T^\dagger} D_z \mathrm{e}^T | \Phi_n \rangle}{\langle \Phi_0 | \mathrm{e}^{T^\dagger} \mathrm{e}^T | \Phi_0 \rangle} \\ &= \frac{\langle \Phi_0 | (T^{(1)^\dagger} \overbrace{D_z^{(0)}} + \overbrace{D_z^{(0)}} T^{(1)}) | \Phi_0 \rangle}{\mathcal{N}_0}, \end{aligned} \tag{16}$$

Table 5. Static dipole polarizabilities in divalent atoms He, Be, Mg, Ca, Sr, Ba and Yb (in a.u.). Results from this work are based on CCSD method and contributions from important triple excitations are given as error bars in parentheses.

Atoms	Expts	Others	This work
He	1.383746(7) [41]	1.383193 [42] 1.389 [33]	1.382(1)
Be		37.755 [43], 37.69 [34], 37.9 [35]	37.8(5)
Mg	71.5(3.1) [44]	71.35 [34], 72.0 [35], 71.3(7) [36]	73(2)
Ca	169(17) [44]	159.4 [34], 152.7 [44], 157.1(1.3) [36] 152 [45], 158.0 [37]	155(5)
Sr	186(15) [44]	201.2 [34], 193.2 [35], 197.2(2) [36] 190 [45], 198.9 [37]	200(7)
Ba	268(22) [46]	264 [38], 273 [45], 273.9 [37]	268(9)
Yb	142(36) [47]	111.3(5) [36], 141.7 [48], 157.30 [39]	144(6)

where for computational simplicity we define $\widetilde{D_z^{(0)}} = \mathrm{e}^{T^{(0)^\dagger}} D_z \mathrm{e}^{T^{(0)}}$ and the norms of the wave functions are given by $\mathcal{N}_0 = \langle\Phi_0|\mathrm{e}^{T^{(0)^\dagger}}\mathrm{e}^{T^{(0)}}|\Phi_0\rangle$. We compute these terms by expressing as effective one-body and two-body terms using the generalized Wick's theorem.

In table 5, we present our results of electric dipole polarizabilities for various atoms and compare them with the available experimental results. We have considered lighter atoms including He to make sure that our new approach is also giving reasonably good results compared to their experimental results. Then the method has been employed to calculate these properties in Ba and Yb. From the error bars in parantheses from the perturbed triple excitation contributions, it is clear that these contributions are becoming important for heavy atoms.

To emphasize the importance of correlation effects in these calculations, we present the DF and the leading RCC contributions in table 6 for the electric dipole polarizabilities. For all the cases considered, the DF results are larger than the total results. From the individual RCC contributions, we find that only the terms arising from $\overline{D_z}T_1^{(1)}$ and its conjugate (cc) are significant. Given that these terms include the DF, leading core polarization and other important correlation effects to all orders, it is not surprising that they should collectively make up the largest contribution.

6. Calculations of atomic properties of Yb

6.1 *The* $5d6s\ ^3D_J$–$6s6p\ ^3P_J$ *electric dipole transitions*

The $5d6s\ ^3D_1$–$6s^2\ ^1S_0$ $M1$ transition amplitude is an important quantity of interest for the ongoing Yb atomic parity non-conservation experiments. The semi-empirical

Table 6. Contributions from DF and important perturbed CC terms (in a.u.) for the considered atoms.

Atoms	DF	$(\widehat{D_z}\,T_1^{(1)}+\text{cc})-\text{DF}$	$\widehat{D_z}\,T_2^{(1)}+\text{cc}$	$\mathcal{N}_0$
He	1.495	−0.12	0.005	−0.1E-4
Be	45.82	−7.94	−0.09	0.02
Mg	82.44	−8.77	−0.21	0.03
Ca	184.14	−29.23	−0.07	−0.26
Sr	234.41	−34.46	−0.17	−0.08
Ba	328.32	−61.18	0.09	0.81
Yb	183.32	−39.86	0.032	1.10

[3] values are in agreement with the experimentally measured value [17] of the transition amplitude. However, there are no theoretical calculations. As a step towards the theoretical calculation of the $M1$ transition, the $E1$ transition between $5d6s\ ^3D_J$ and $6s6p\ ^3P_J$ multiplets were studied to test the accuracy of the atomic states calculated.

6.2 *The ac Stark shift of* $5d6s\ ^3D_1$ *level*

In the parity non-conservation experiment, a strong laser field of 408 nm drives the $5d6s\ ^3D_1$–$6s^2\ ^1S_0$ transition. This induces ac Stark shift to the levels and can add to the uncertainty in the measured E1PNC. An interesting feature of the $5d6s\ ^3D_1$ ac Stark shift is the presence of odd-parity $6snp$ levels nearly resonant to the applied laser field. This can produce large ac Stark shift to $5d6s\ ^3D_1$, but experimental results show otherwise [18]. A theoretical study can perhaps provide an insight into the effect of near-resonant $6snp$ states.

The ac Stark shift or the light shift of an atomic state $|\Psi_i\rangle$ in a laser of frequency ω and intensity I is

$$\Delta E(\omega) = \frac{I}{2}\sum_j \frac{\Delta E_{ij}|\langle\Psi_i|\mathbf{r}_{ij}|\Psi_j\rangle|^2}{\Delta E_{ij}^2-\omega^2}, \tag{17}$$

where $\mathbf{r}_{ij}$ is the dipole transition matrix element between the ith state and opposite parity intermediate jth states, and $\Delta E_{ij} = E_i - E_j$ is the energy difference. In the expression, the matrix element $\langle\Psi_i|\mathbf{r}_{ij}|\Psi_j\rangle$ can be calculated either theoretically or from the experimental data. The calculation from the experimental data is difficult when there are several decay channels, which is true of high-lying states like the near-resonant $6snp$ states. Theoretically, an estimate of $\langle\Psi_i|\mathbf{r}_{ij}|\Psi_j\rangle$ can be made using the multi-configuration Dirac–Fock wave functions of the $6snp$ states. For the ac Stark shift of $5d6s\ ^3D_1$, the dominant single-particle matrix elements are $|6s|\mathbf{r}|np\rangle|$. The radial component of the single-particle matrix elements are given in table 7. It is also possible to calculate the radial matrix elements semi-empirically using Bates–Damgaard approximation [49]. It is a central field core approximation and the radial matrix element is a function of the effective quantum number n^*.

Table 7. The single electron radial matrix elements. The n^* are the effective principal quantum number calculated from the experimental data, which are used in the BD approximation to calculate radial dipole matrix elements. The BD value and MCDF value are the matrix elements calculated using BD approximation and MCDF wave functions respectively.

Matrix element	n^*	BD value	MCDF value
$\langle 6s\|d\|6p\rangle$	1.43	1.82	−4.29
$\langle 6s\|d\|7p\rangle$	1.81	2.44	−0.94
$\langle 6s\|d\|8p\rangle$	1.97	2.40	−0.46
$\langle 6s\|d\|9p\rangle$	2.06	2.25	−0.29
$\langle 6s\|d\|10p\rangle$	2.12	2.10	−0.21
$\langle 6s\|d\|11p\rangle$	2.15	2.02	−0.16
$\langle 6s\|d\|12p\rangle$	2.18	1.93	−0.13
$\langle 6s\|d\|13p\rangle$	2.20	1.87	−0.11

The BD approximation of the radial matrix elements are given in table 7. There is a large discrepancy between the MCDF values and BD approximation results, and except $\langle 6s|d|6p\rangle$ the BD matrix elements are an order of magnitude larger than the MCDF results. The possible reason is the low value of n^* calculated from the experimental data, usually $n - 5 \geq n^* \leq n - 4$. It is found that n^* calculated from the theoretical np ionization energies yields BD matrix elements which are in agreement with the MCDF values. This shows the method is not suitable for Yb because of the large ionization threshold energy, which is an indication of strong correlation effects and inaccuracy of a central field approximation of the valence shells.

From the calculations, the contribution from the near-resonant $6snp$ to the $5d6s\ ^3d_1$ ac Stark shift is negligible. The dipole matrix elements are an order of magnitude smaller than the most dominant $6s6p$ states and there are cancellations between the $6snp$ states on opposite sides of the resonance position. Thus, in the 408 nm laser field only the $6s^2\ ^1S_0$ ac Stark shift affects the $5d6s\ ^3D_1$–$6s^2\ ^1S_0$ transition.

7. Conclusion

An overview of certain experimental and theoretical aspects of violations of fundamental symmetries in atoms has been presented. Experimental techniques to measure parity violation in ytterbium and dysprosium and test the violation of Bose statistics by photons are discussed. Theoretical studies on some of the properties related to parity violation in ytterbium have been performed and a new theoretical approach has been developed to estimate the static dipole polarizabilities of closed-shell atoms. Theoretical work on parity violation in ytterbium is currently in progress.

Acknowledgements

We acknowledge the invaluable contributions of Jason Stalnaker, Nathan Leefer, Arijit Sharma, Damon English, Konstantin Tsigutkin, Sadiqali Rangwala, Dimitri Dounas-Frazer, Victor Acosta, Derek Jackson Kimball, Simon Rochester and Brajesh Mani. This work has been supported in part by the NSF-DST International Collaboration Grant OISE-0425916, NSF Grant PHY-0758031, and by the U.S. Department of Energy, Office of Basic Energy Sciences, Division of Nuclear Science under Contract No. DE-AC02-05CH11231.

References

[1] D Budker, *WEIN 1998 Proceedings* edited by P Herczeg, C M Hoffman and H V Klapdor-Kleingrothus (World Scientific, Singapore, 1999)
[2] M A Bouchiat and C Bouchiat, *J. Phys. (Paris)* **35**, 899 (1974)
[3] D DeMille, *Phys. Rev. Lett.* **74**, 4165 (1995)
[4] B P Das, *Phys. Rev.* **A56**, 1635 (1997)
[5] S G Porsev, G Rakhlina Yu and M G Kozlov, *JETP Lett.* **61**, 459 (1995)
[6] K Tsigutkin, D Dounas-Frazer, A Family, J E Stalnaker, V V Yashchuk and D Budker, *Phys. Rev. Lett.* **103**, 071601 (2009)
[7] K Tsigutkin, D Dounas-Frazer, A Family, J E Stalnaker, V V Yashchuk and D Budker, *Phys. Rev.* **A81**, 032114 (2010)
[8] A-T Nguyen, D Budker, D DeMille and M Zolotorev, *Phys. Rev.* **A56**, 3453 (1997)
[9] V A Dzuba, V V Flambaum and M V Marchenko, *Phys. Rev.* **A68**, 022506 (2003)
[10] A Cingoz, A Lapierre, A-T Nguyen, N Leefer, D Budker, S K Lamoreaux and J R Torgerson, *Phys. Rev. Lett.* **98**, 040801 (2007)
[11] L D Landau, *Sov. Phys. Doklady* **60**, 207 (1948)
[12] C N Yang, *Phys. Rev.* **77**, 242 (1950)
[13] D DeMille, D Budker, N Derr and E Deveney, *Phys. Rev. Lett.* **83**, 3978 (1999)
[14] D Angom, Kaushik Bhattacharya and Saurabh D Rindani, *Int. J. Mod. Phys.* **A22**, 707 (2007)
[15] Angom D Singh and B P Das, *J. Phys.* **B32**, 4905 (1999)
[16] B K Mani and D Angom, arXiv:1009.2963
[17] J E Stalnaker, D Budker, D P DeMille, S J Freedman and V V Yashchuk, *Phys. Rev.* **A66**, 031403 (2002)
[18] J E Stalnaker, *Progress towards parity conservation in atomic ytterbium*, Ph.D. Thesis (University of California, Berkeley, 2005)
[19] B A Brown, A Derevianko and V V Flambaum, *Phys. Rev.* **C79**, 035501 (2009)
[20] V A Dzuba, V V Flambaum and I B Khriplovich, *Z. Phys.* **D1**, 243 (1986)
[21] V A Dzuba and V V Flambaum, *Phys. Rev.* **A81**, 052515 (2010)
[22] A Cingz, N A Leefer, S J Ferrell, A Lapierre, A-T Nguyen, V V Yashchuk, D Budker, S K Lamoreaux and J R Torgerson, *Eur. Phys. J. Special Topics* **163**, 71 (2008)
[23] S J Ferrell, A Cingoz, A Lapierre, A-T Nguyen, N Leefer, D Budker, V V Flambaum, S K Lamoreaux and J R Torgerson, *Phys. Rev.* **A76**, 062104 (2007)
[24] A-T Nguyen, G D Chern, D Budker and M Zolotorev, *Phys. Rev.* **A63**, 013406 (2001)
[25] N Leefer, A Cingz, B Gerber-Siff, Arijit Sharma, J R Torgerson and D Budker, *Phys. Rev.* **A81**, 043427 (2010)
[26] N A Leefer, A Cingz and D Budker, *Opt. Lett.* **34**, 2548 (2009)

[27] N A Leefer, A Cingz, D Budker, S J Ferrell, V V Yashchuk, A Lapierre, A-T Nguyen, S K Lamoreaux and J R Torgerson, *Proceedings of the 7th Symposium: Frequency Standards and Metrology*, Asilomar, October 2008; edited by Lute Maleki (World Scientific; elSBN: 9789812838223) pp. 34–43
[28] Damon English, Valeriy V Yashchuk and Dmitry Budker, *Phys. Rev. Lett.* **104**, 253604 (2010)
[29] M G Kozlov, D Budker and D English, *Phys. Rev.* **A80**, 042504 (2009)
[30] T K Chyi, C W Hwang, W F Kao, G L Lin, K W Ng and J J Tseng, *Phys. Rev.* **D62**, 105014 (2000)
[31] F A Parpia, C Froese Fischer and I P Grant, *Comp. Phys. Comm.* **94**, 249 (1996)
[32] A Dalgarno and Lewis, *Proc. R. Soc.* **A233**, 70 (1955)
[33] Z W Liu and H P Kelly, *Theor. Chim. Acta* **80**, 307 (1991)
[34] J Mitroy and M W J Bromley, *Phys. Rev.* **A68**, 052714 (2003)
[35] S H Patil, *J. Phys.* **D10**, 341 (2000)
[36] S G Porsev and A Derevianko, *Phys. Rev.* **A74**, 020502(R) (2006)
[37] I S Lim and P Schwerdtfeger, *Phys. Rev.* **A70**, 062501 (2004)
[38] M G Kozlov and S G Porsev, *Eur. Phys. J.* **D5**, 59 (1999)
[39] X Chu, A Dalgarno and G C Groenenboom, *Phys. Rev.* **A75**, 032723 (2007)
[40] B K Sahoo and B P Das, *Phys. Rev.* **A77**, 062516 (2008)
[41] K Grohman and H Luther, *Temperature – Its measurement and control in science and industry* (AIP, New York, 1992) Vol. 6, p. 21
[42] M Masili and A F Starace, *Phys. Rev.* **A68**, 012508 (2003)
[43] J Komasa, *Phys. Rev.* **A65**, 012506 (2001)
[44] T M Miller, *Atomic and molecular polarizabilities* (CRC Press, Boca Raton, Florida, 1995) Vol. 76, p. 10; 020502(R) (2006)
[45] A J Sadlej, M Urban and O Gropen, *Phys. Rev.* **A44**, 5547 (1991)
[46] H L Schwartz, T M Miller and B Bederson, *Phys. Rev.* **A10**, 1924 (1974)
[47] T M Miller, *CRC handbook of chemistry and physics*, 77th edition, edited by D R Lide (CRC, Boca Raton, 1996)
[48] A A Buchachenko, M M Szczesniak and G Chalasinski, *J. Chem. Phys.* **124**, 114301 (2006)
[49] I I Sobelman, *Atomic spectra and radiative transitions*, 2nd edition (Springer-Verlag, 1991)